Please cite this paper as: J. M. Aristoff, J. T. Horwood, N. Singh, and A. B. Poore, "Nonlinear uncertainty propagation in orbital elements and transformation to Cartesian space without loss of realism," in Proceedings of the 2014 AAS/AIAA Astrodynamics Specialist Conference, San Diego, CA, August 2014 (Paper AIAA-2014-4167)

Nonlinear Uncertainty Propagation in Orbital Elements and Transformation to Cartesian Space Without Loss of Realism

Jeffrey M. Aristoff*, Joshua T. Horwood†, Navraj Singh‡ and Aubrey B. Poore§

Numerica Corporation, Fort Collins, Colorado, 80528, USA

A number of methods for nonlinear uncertainty propagation used for space situational awareness (SSA) exploit orbital-element-based representations of orbital-state uncertainty in order to mitigate the departure from Gaussianity and thereby improve performance. However, some downstream SSA functions require that orbital-state uncertainty be represented in a Cartesian space. This paper reconciles the two practices by describing a way in which uncertainty that has been propagated in orbital elements can be transformed to Cartesian space without loss of realism via Gaussian mixtures. The efficiency of this approach is compared to an alternative approach to uncertainty propagation wherein uncertainty is both represented and propagated in Cartesian space (using Gaussian mixtures). Metrics for assessing the realism of a Gaussian mixture are also presented.

I. Introduction

An unbiased and consistent characterization of the errors in the state of a space object (i.e., covariance and uncertainty realism) is needed for many space situational awareness (SSA) functions (e.g., tracking, conjunction analysis, sensor tasking and scheduling, etc.). Indeed, in response to the National Research Council's recent assessment of Air Force Space Command's Astrodynamics Standards,[1] the Astrodynamics Innovation Committee established a Covariance Realism Working Group to define, assess, and improve covariance and uncertainty realism. In the context of uncertainty propagation, highly nonlinear dynamics and long propagation times present serious challenges and often require the use of computationally expensive methods for propagation (e.g., particle filters[2] or Gaussian mixture filters[3,4,5,6,7,8]) in order to maintain covariance (and uncertainty) realism, even if one were to perfectly model the dynamics.

A recent breakthrough in the propagation and representation of orbital state uncertainty enables covariance (and uncertainty) realism to be maintained for up to 32 times longer than traditional methods of comparable computational cost.[9] Such benefits were quantified using powerful and well-poised distribution matching tests based on the Mahalanobis distance and its generalization to non-Gaussian distributions,[10] and a Gaussian probability density function at epoch was assumed. Improved performance is achieved by combining two complementary approaches: (i) the use of a newly-developed system of (non-singular) orbital elements tailored to the underlying dynamics that more closely preserve Gaussian and linear assumptions,[11] and (ii) the use of the prediction step of the Gauss von Mises (GVM) filter to rigorously treat uncertainty in orbital element space and model higher-order cumulants beyond a state and covariance.[12,13] Further improvements in runtime and accuracy can be achieved via the use of highly-stable implicit-Runga-Kutta-based numerical integration techniques that have been specialized for uncertainty propagation.[14,15,16]

In this paper, we demonstrate how uncertainty in orbital elements can be faithfully transformed to Cartesian space as required for some downstream SSA functions (e.g., traditional methods for conjunction

*Senior Research Scientist, Numerica Corporation, 5042 Technology Parkway, Suite 100, Fort Collins, Colorado, 80528.
†Program Manager, Numerica Corporation.
‡Research Scientist, Numerica Corporation.
§Chief Scientific Officer, Numerica Corporation.

analysis that require the covariance in Cartesian space at closest approach). Although our approach is applicable to other probability density functions (e.g., GVM distributions), attention will be restricted to the most common case in which the uncertainty is represented by a multi-variate Gaussian or mixture thereof. This transformation entails (i) refining the probability density function in orbital elements into a Gaussian mixture in orbital elements, (ii) converting each component of the Gaussian mixture to Cartesian space, and (iii) assessing the realism of said transformation and further refining the distribution if necessary. The resulting mixture distribution can then be easily used for scoring association hypotheses or for computing probabilities of collision, etc.

Further, the above approach is compared and contrasted to an alternative approach for uncertainty propagation wherein the uncertainty is kept in Cartesian space and propagated using Gaussian mixtures. Specifically, we quantify how many Gaussian mixture components would be needed to properly characterize uncertainty in Cartesian space as a function of initial state, covariance, and propagation time using realistic dynamical models. It is demonstrated that the computational cost of uncertainty propagation can be reduced by several orders of magnitude via the above approach.

The layout of this paper is as follows. Section II presents a method for refining a Gaussian distribution in orbital elements into a Gaussian mixture distribution in Cartesian space, including metrics for assessing said transformation (i.e., the realism of the resulting Gaussian mixture). Section III demonstrates the efficacy of the approach when applied to the propagation of both low- and high-accuracy orbits in multiple regimes of space. Section IV provides concluding remarks.

II. Methods and Assumptions

The effectiveness of nonlinear filters and uncertainty propagation algorithms can be significantly enhanced through the use of appropriate coordinate systems tailored to the underlying dynamics.[9] For example, equinoctial orbital elements[17] absorb the most dominant term in the nonlinear dynamics (i.e., the $1/r^2$ term in the gravitational force), thereby more closely preserving any Gaussian and linear approximations. In other words, uncertainty realism can be maintained for significantly longer propagation times when the space object's state uncertainty is represented in equinoctial orbital elements compared to Cartesian representations. Further improvements are possible by incorporating higher-order perturbations beyond the $1/r^2$ contribution. Indeed, we have developed a new system of orbital elements, called the J_2 equinoctial orbital elements, that effectively absorb the J_2 zonal perturbation (i.e., the second-most dominant term in the geopotential expansion that accounts for the Earth's oblateness).[11] Note that unlike the classical Keplerian orbital elements, the traditional equinoctial orbital elements and the J_2 equinoctial orbital elements are non-singular for orbits with zero eccentricity or zero inclination.

The purpose of this section is not to present a derivation of the J_2 equinoctial orbital elements nor demonstrate their efficacy in the context of nonlinear uncertainty propagation. Rather, the remainder of this section describes how to transform a Gaussian (or Gaussian mixture) in orbital element space to a Gaussian mixture in Cartesian space without loss of realism, as is needed to meet the interface requirements for some space surveillance systems. Without loss of generality, we restrict our attention to the refinement of a single Gaussian; refinement of a Gaussian mixture can be performed in parallel on each Gaussian component.

A. Mathematical Preliminaries

A random vector $\boldsymbol{x} \in \mathbb{R}^n$ is said to be distributed as a Gaussian mixture if and only if its probability density function (PDF) is of the form

$$p_x\left(\boldsymbol{x}; \left\{w_i, \boldsymbol{\mu}_i, \mathbf{P}_i\right\}_{i=1}^{N}\right) = \sum_{i=1}^{N} w_i \mathcal{N}(\boldsymbol{x}; \boldsymbol{\mu}_i, \mathbf{P}_i),$$

where the given weights w_i, $i = 1, \ldots, N$, are non-negative scalars which sum to unity, and $\mathcal{N}(\boldsymbol{x}; \boldsymbol{\mu}, \mathbf{P})$ denotes the Gaussian PDF with the mean vector $\boldsymbol{\mu}$ and the symmetric positive-definite covariance matrix $\mathbf{P}$; i.e.,

$$\mathcal{N}(\boldsymbol{x}; \boldsymbol{\mu}, \mathbf{P}) = \frac{1}{\sqrt{\det(2\pi\mathbf{P})}} \exp\left[-\frac{1}{2}(\boldsymbol{x}-\boldsymbol{\mu})^T \mathbf{P}^{-1}(\boldsymbol{x}-\boldsymbol{\mu})\right]. \tag{1}$$

A fundamental result of Alspach and Sorenson[18] providing the theoretical foundations of this work states that any PDF can be approximated arbitrarily close (in the L_1 sense) by a Gaussian mixture[a].

B. Refinement of a Gaussian into a Gaussian mixture

The objective of refinement, sometimes called splitting, is to approximate a given Gaussian PDF $\mathcal{N}(\boldsymbol{x}; \boldsymbol{\mu}, \mathbf{P})$ by a Gaussian mixture PDF according to

$$\mathcal{N}(\boldsymbol{x}; \boldsymbol{\mu}, \mathbf{P}) \approx \sum_{i=1}^{N} w_i \mathcal{N}(\boldsymbol{x}; \boldsymbol{\mu} + k_i \boldsymbol{u}; \mathbf{P}_i), \tag{2}$$

where $\boldsymbol{u}$ is a specified unit vector called the refinement direction. The parameters w_i, k_i, and $\mathbf{P}_i$, for $i = 1, \ldots, N$, are computed from an optimization principle described later in this subsection. Refinement is a critical component of any implementation of a Gaussian mixture filter (sometimes called a Gaussian sum filter). Indeed, in a sufficiently small neighborhood, any (smooth) nonlinear transformation is approximately linear. Consequently, Gaussians with smaller covariances (i.e., the mixture components) remain more Gaussian than those with a larger covariance (i.e., the input Gaussian) under a nonlinear map. In other words, a Gaussian refined into a Gaussian mixture exhibits better behavior through a nonlinear transformation (e.g., transformation between orbital elements and Cartesian space). The refinement direction $\boldsymbol{u}$ (along which the component means of the mixture are located) is usually chosen to coincide with the direction in which the nonlinearity is most severe.

In order to determine the parameters in the refinement (2), the discussions of this subsection are organized as follows.

1. Algorithm 1 is stated which describes the solution to the refinement problem for the special case when the input is the univariate standardized Gaussian.
2. Algorithm 2 is derived which describes the solution to the refinement problem for the general case of a multivariate Gaussian using an arbitrary refinement direction $\boldsymbol{u}$.
3. Methods for selecting the refinement direction $\boldsymbol{u}$ are suggested.

A prerequisite to refining a multivariate Gaussian PDF is the refinement of the univariate standardized Gaussian into a Gaussian mixture:

$$\mathcal{N}(x; 0, 1) \approx \sum_{i=1}^{N} w_i \mathcal{N}(x; \mu_i, \sigma_i^2).$$

For fixed N, the component weights w_i, means μ_i, and standard deviations σ_i can be computed by solving the following L_2 optimization problem:

$$\begin{aligned} \underset{\substack{w_1,\ldots,w_N \\ \mu_1,\ldots,\mu_N \\ \sigma_1,\ldots,\sigma_N}}{\text{Minimize}} \quad & E \\ \text{Subject to} \quad & \sum_{i=1}^{N} w_i = 1, \quad w_i \geq 0, \quad i = 1, \ldots, N, \\ & \mu_1 \leq \mu_2 \leq \cdots \leq \mu_N, \\ & \sigma_i \leq \sigma < 1, \quad i = 1, \ldots, N. \end{aligned} \tag{3}$$

where the objective function

$$\begin{aligned} E &= \int_{-\infty}^{\infty} \left[\mathcal{N}(x; 0, 1) - \sum_{i=1}^{N} w_i \mathcal{N}(x; \mu_i, \sigma_i^2) \right]^2 \mathrm{d}x \\ &= \boldsymbol{w}^T \mathbf{M} \boldsymbol{w} - 2\boldsymbol{w}^T \boldsymbol{n} + \frac{1}{2\sqrt{\pi}}, \end{aligned}$$

[a] If the underlying space is finite, then L_2 is contained in L_1. Because the PDFs we are dealing with decay exponentially, a finite approximation is reasonable and refinement in an L_2 sense provides a good approximation.[5]

Algorithm 1: Refinement of the Univariate Standardized Gaussian

Approximation of the univariate standardized Gaussian $\mathcal{N}(x;0,1)$ *by a Gaussian mixture* $\sum_{i=1}^{N} w_i \mathcal{N}(x;\mu_i,\sigma_i^2)$.

input : refinement parameter $\sigma \in (0,1)$
output: parameter set $\{w_i,\mu_i,\sigma_i^2\}_{i=1}^N$ of the approximating Gaussian mixture

begin
  if $\sigma \geq \frac{2}{3}$ **then**
    $N \leftarrow 3$
    Generate $\{w_i,\mu_i,\sigma_i^2\}_{i=1}^N$ from Table 1
    return
  if $\sigma \geq \frac{1}{2}$ **then**
    $m \leftarrow 4$
    $\sigma \leftarrow \frac{1}{2}$
  else
    $m \leftarrow 6$
  $N \leftarrow \lceil 1 + 2m/\sigma \rceil$
  for $i \leftarrow 1$ **to** N **do**
    $\mu_i \leftarrow -m + \sigma(i-1)$
    $\sigma_i \leftarrow \sigma$
  Solve the constrained quadratic programming program $\boldsymbol{w} \leftarrow \arg\min_{\boldsymbol{w}} \boldsymbol{w}^T\mathbf{M}\boldsymbol{w} - 2\boldsymbol{w}^T\boldsymbol{n}$ subject to $\sum_{i=1}^N w_i = 1$ and $w_i \geq 0$, for $i = 1,\ldots,N$, where the components of $\boldsymbol{w}$, $\boldsymbol{n}$, and $\mathbf{M}$ are defined by Equations (4).
  for $i \leftarrow 1$ **to** N **do**
    $w_i \leftarrow (\boldsymbol{w})_i$

and where

$$(\boldsymbol{w})_i = w_i, \quad (\boldsymbol{n})_i = \mathcal{N}(\mu_i;0,\sigma_i^2+1), \quad (\mathbf{M})_{ij} = \mathcal{N}(\mu_i-\mu_j;0,\sigma_i^2+\sigma_j^2). \tag{4}$$

How the user-defined parameter $\sigma \in (0,1)$ is chosen is discussed momentarily. Solving the constrained nonlinear optimization problem above is computationally challenging. (It is not a quadratic programming problem since the matrix $\mathbf{M}$ in the objective function depends on the unknown means and standard deviations.) Some additional insights are provided in Reference 5. A solution derived by DeMars[19] for the case $N = 3$ is provided in Table 1. Horwood *et al.*[5] argue that a sub-optimal approach which fixes the component means and standard deviations according to a prescribed formula produces a reasonable solution with L_2 errors as small as 10^{-8} for $N \gtrapprox 100$. In such a case, the constrained minimization of the L_2 error reduces to a computationally tractable quadratic programming problem. This is provided as Algorithm 1.

Table 1. Refinement of the univariate standardized Gaussian into a Gaussian mixture with $N = 3$ components.

i	w_i	μ_i	σ_i
1	0.225224624913675	-1.057515461475881	0.671566288664076
2	0.549550750172650	0	0.671566288664076
3	0.225224624913675	1.057515461475881	0.671566288664076

In the multivariate case, the input Gaussian PDF $\mathcal{N}(\boldsymbol{x};\boldsymbol{\mu},\mathbf{P})$ in (2) is refined into components whose means lie along a particular refinement direction. In Reference 5, the refinement direction is assumed to be along a canonical basis vector, while DeMars[19] restricts the refinement direction to be along an eigenvector of the input covariance matrix $\mathbf{P}$. The extension of these methods to refinement in the direction of an arbitrary unit vector $\boldsymbol{u}$ can be achieved as follows. Firstly, Algorithm 1 is applied with a prescribed $\sigma \in (0,1)$ as the input where the output is denoted as $\{\tilde{w}_i,\tilde{k}_i,\tilde{\sigma}_i^2\}_{i=1}^N$ which describes the parameter set of the Gaussian mixture approximating the univariate standardized Gaussian. This parameter set is used to construct a Gaussian mixture approximation of the n-dimensional standardized Gaussian with refinement along the canonical basis vector $\boldsymbol{e}_1 = (1,0,\ldots,0)^T$:

$$\mathcal{N}(\boldsymbol{z};\mathbf{0},\mathbf{I}) \approx \sum_{i=1}^{N} \tilde{w}_i \mathcal{N}(\boldsymbol{z};\tilde{k}_i\boldsymbol{e}_1,\tilde{\mathbf{P}}_i). \tag{5}$$

Algorithm 2: Refinement of a Multivariate Gaussian

Approximation of a multivariate Gaussian $\mathcal{N}(\boldsymbol{x};\boldsymbol{\mu},\mathbf{P})$ by a Gaussian mixture $\sum_{i=1}^{N} w_i \mathcal{N}(\boldsymbol{x};\boldsymbol{\mu}+k_i\boldsymbol{u},\mathbf{P}_i)$ with refinement along a prescribed unit vector $\boldsymbol{u}$.

inputs : refinement parameter $\sigma \in (0,1)$; mean-covariance pair $(\boldsymbol{\mu},\mathbf{P})$;
unit vector $\boldsymbol{u}$ describing the refinement direction

output: parameter set $\{w_i,\boldsymbol{\mu}+k_i\boldsymbol{u},\mathbf{P}_i\}_{i=1}^{N}$ of the approximating Gaussian mixture

begin
- $\{\tilde{w}_i,\tilde{k}_i,\tilde{\sigma}_i^2\}_{i=1}^{N} \leftarrow$ Algorithm 1(σ)
- $\tilde{\boldsymbol{u}} \leftarrow \mathbf{A}^{-1}\boldsymbol{u}/\|\mathbf{A}^{-1}\boldsymbol{u}\|_2$, where $\mathbf{A}$ is the lower-triangular Cholesky factor of $\mathbf{P}$
- $\boldsymbol{\Lambda} \leftarrow \mathbf{Q}$, where $\mathbf{Q}$ is an orthogonal matrix resulting from a QR-factorization of $\tilde{\boldsymbol{u}}$
- **for** $i \leftarrow 1$ **to** N **do**
  - $\tilde{\mathbf{P}}_i \leftarrow \mathrm{diag}(\tilde{\sigma}_i^2,1,\ldots,1)$
  - $w_i \leftarrow \tilde{w}_i$
  - $k_i \leftarrow \tilde{k}_i/\|\mathbf{A}^{-1}\boldsymbol{u}\|_2$
  - $\mathbf{P}_i \leftarrow \mathbf{A}\boldsymbol{\Lambda}^T\tilde{\mathbf{P}}_i\boldsymbol{\Lambda}\mathbf{A}^T$

In the above expression, $\tilde{\mathbf{P}}_i = \mathrm{diag}(\tilde{\sigma}_i^2,1,\ldots,1)$. Secondly, an orthogonal matrix (rotation) $\boldsymbol{\Lambda}$ is determined such that $\boldsymbol{\Lambda}\tilde{\boldsymbol{u}} = \boldsymbol{e}_1$, where $\tilde{\boldsymbol{u}}$ is the unit vector $\mathbf{A}^{-1}\boldsymbol{u}/\|\mathbf{A}^{-1}\boldsymbol{u}\|_2$ and $\mathbf{A}$ is the lower-triangular Cholesky factor of $\mathbf{P}$ such that $\mathbf{P} = \mathbf{A}\mathbf{A}^T$. Such a matrix $\boldsymbol{\Lambda}$ can be computed, for example, by performing a QR-factorization of $\tilde{\boldsymbol{u}}$; $\boldsymbol{\Lambda}$ is the orthogonal matrix $\mathbf{Q}$. Lastly, the change of variables $\boldsymbol{x} = \boldsymbol{\mu} + \mathbf{A}\boldsymbol{\Lambda}^T\boldsymbol{z}$ is performed to both sides of (5). This yields the following Gaussian mixture approximation with respect to $\boldsymbol{x}$:

$$\mathcal{N}(\boldsymbol{x};\boldsymbol{\mu},\mathbf{P}) \approx \sum_{i=1}^{N} \tilde{w}_i \mathcal{N}(\boldsymbol{x};\boldsymbol{\mu}+\tilde{k}_i\mathbf{A}\boldsymbol{\Lambda}^T\boldsymbol{e}_1, \mathbf{A}\boldsymbol{\Lambda}^T\tilde{\mathbf{P}}_i\boldsymbol{\Lambda}\mathbf{A}^T).$$

By construction, $\boldsymbol{\Lambda}^T\boldsymbol{e}_1 = \tilde{\boldsymbol{u}}$ and $\mathbf{A}\tilde{\boldsymbol{u}} = \boldsymbol{u}/\|\mathbf{A}^{-1}\boldsymbol{u}\|_2$; hence the component means in the above Gaussian mixture approximation are directed along $\boldsymbol{u}$. This achieves the required approximation (2). Algorithm 2 details this procedure.

Both Algorithms 1 and 2 require a parameter $\sigma \in (0,1)$ which controls the relative size of the covariances in the mixture to the size of the covariance of the input. Generally, a smaller σ translates to a smaller L_2 error between the input Gaussian and the output Gaussian mixture and to a Gaussian mixture with a larger number of components N.

One would ideally like to select the refinement direction $\boldsymbol{u}$ so that it coincides with the direction in which the nonlinearity is most severe. When propagating uncertainty in equinoctial orbital elements, the uncertainty in the semi-major axis (radial direction) dominates the growth of the uncertainty along the mean longitude (in-track direction) and potentially causes it to become non-Gaussian. Let $\boldsymbol{v}_i$ for $i = 1\ldots6$ be the eigenvectors of the covariance of the propagated Gaussian distribution in equinoctial (or J_2) orbital elements. We thus choose the refinement vector $\boldsymbol{u}$ so as to maximize $\boldsymbol{v}_i \cdot (0,0,0,0,0,1)$ over i, which is equivalent to choosing the eigenvector with the largest sixth element as the refinement direction. Such a choice can be validated by plotting the final probability density function in semi-major axis and mean longitude subspace.

C. Conversion of each component to Cartesian space

Once the original distribution has been refined into a Gaussian mixture, it is necessary to convert each component from orbital elements to Cartesian space. We next review said transformation. Let $\boldsymbol{\Phi} : \mathbb{R}^n \to \mathbb{R}^n$ be a diffeomorphism (i.e., a bijection on $\mathbb{R}^n$ with a smooth inverse) and define

$$\boldsymbol{y} = \boldsymbol{\Phi}(\boldsymbol{x}).$$

In the context of the present study, $\boldsymbol{\Phi}$ is the function which maps the state of a space object from orbital elements to Cartesian space (i.e., the coordinate transform). By the change of variables theorem, the PDF for $\boldsymbol{y}$ is

$$p_y\left(\boldsymbol{y};\{w_i,\boldsymbol{\mu}_i,\mathbf{P}_i\}_{i=1}^{N}\right) = \left[\det\left(\frac{\partial\boldsymbol{\Phi}}{\partial\boldsymbol{x}}\right)\right]^{-1}_{\boldsymbol{x}=\boldsymbol{\Phi}^{-1}(\boldsymbol{y})} \sum_{i=1}^{N} w_i \mathcal{N}\big(\boldsymbol{\Phi}^{-1}(\boldsymbol{y});\boldsymbol{\mu}_i,\mathbf{P}_i\big). \tag{6}$$

Within the Gaussian mixture framework, the objective is to approximate each component in the mixture (6) by a single Gaussian PDF so that

$$p_y\left(\boldsymbol{y};\left\{w_i,\boldsymbol{\mu}_i,\mathbf{P}_i\right\}_{i=1}^{N}\right)\approx\sum_{i=1}^{N}w_i\,\mathcal{N}(\boldsymbol{y};\tilde{\boldsymbol{\mu}}_i,\tilde{\mathbf{P}}_i). \tag{7}$$

The transformed components $\tilde{\boldsymbol{\mu}}_i$ and $\tilde{\mathbf{P}}_i$ in (7) can be computed using, for example, the unscented transform (or higher-order Gauss-Hermite quadrature) of the unscented Kalman filter (UKF).[20] Additional details on the application of the UKF within a Gaussian mixture filter are described in References 5, 6, 7, 8 and 19. Optionally, one could adjust the weights and the number of components[4] but such techniques will not be considered here. If the component covariances $\mathbf{P}_i$ in (6) are sufficiently small, then $\boldsymbol{\Phi}$ will be approximately linear in each of their respective neighborhoods; hence each mixture component component will be well-approximated by a single Gaussian[b]. The metrics defined in the next subsection provide a means for validating the approximation (7) by generalizing the Mahalanobis distance to non-Gaussian distributions.

D. Metrics for assessing the realism of a Gaussian mixture

Let $p_x(\boldsymbol{x};\boldsymbol{\Theta})$ denote a general PDF in the n-dimensional orbit state $\boldsymbol{x}$ with some parameter set $\boldsymbol{\Theta}$. The generalization of the Mahalanobis distance which serves as a metric for *uncertainty realism* is defined by

$$\mathcal{U}(\boldsymbol{x};\boldsymbol{\Theta})=-2\ln\left[\frac{p_x(\boldsymbol{x};\boldsymbol{\Theta})}{p_x(\hat{\boldsymbol{x}};\boldsymbol{\Theta})}\right], \tag{8}$$

where $\hat{\boldsymbol{x}}$ is the mode of $\boldsymbol{x}$:

$$\hat{\boldsymbol{x}}=\arg\max_{\boldsymbol{x}}\ p_x(\boldsymbol{x};\boldsymbol{\Theta}).$$

We remark that for a Gaussian PDF, as defined in (1), the parameter set $\boldsymbol{\Theta}$ encapsulates the mean $\boldsymbol{\mu}$ and covariance $\mathbf{P}$. Further, in such a case, the uncertainty realism metric (8) reduces to

$$\mathcal{U}(\boldsymbol{x};\boldsymbol{\Theta})=\mathcal{U}(\boldsymbol{x};\boldsymbol{\mu},\mathbf{P})=(\boldsymbol{x}-\boldsymbol{\mu})^T\mathbf{P}^{-1}(\boldsymbol{x}-\boldsymbol{\mu}),$$

which is precisely the (square of the) Mahalanobis distance.[21] Additional details regarding the uncertainty realism metric and situations in which it is chi-squared distributed are provided in Reference 10. A description of its use in conjunction with the Cramér-von Mises goodness-of-fit test is given in Section III, Subsection A.

III. Results and Discussion

In previous work (see Reference 9), we presented a unified testing framework for assessing uncertainty realism during nonlinear uncertainty propagation under the perturbed two-body problem of celestial mechanics, as well as a suite of metrics and benchmark test cases on which to validate different methods. Comparison was made between different combinations of uncertainty propagation techniques and coordinate systems for representing uncertainty, and the propagation time after which uncertainty realism breaks down was quantified for each of the test cases, a summary of which is given in Figure 1.

In the aforementioned study, only the prediction steps of single-component nonlinear filters were considered, i.e., that of the unscented Kalman filter (UKF), extended Kalman filter (EKF), and Gauss von Mises filter (GVM). Hence, a natural question arises. How many mixture components in a mixture version of the aforementioned filters would be needed to properly characterize the uncertainty in a space object's orbital state for a given propagation time? In this section, we answer this question by propagating uncertainty in J_2 equinoctial orbital elements and converting the final distribution to both traditional equinoctial orbital elements and Cartesian space. In doing so, we demonstrate the aforementioned approach to nonlinear uncertainty propagation, i.e., propagation in orbital elements and transformation to Cartesian space without loss of realism via Gaussian mixtures. Computational considerations are also discussed.

[b]The approximation in (7) is exact if $\boldsymbol{\Phi}$ is linear or in the limit as $\|\mathbf{P}_i\|\to 0$, for $i=1,\ldots,N$.

	ECI	EqOE	J_2EqOE
EKF	0.3	1.2	5.8
UKF	0.3	1.3	8.4
GVM-3	N/A	2.7	9.5
GVM-5	N/A	4.5	9.5

(a) Scenario 1 (low-accuracy LEO)

	ECI	EqOE	J_2EqOE
EKF	0.3	1.1	4.8
UKF	0.3	1.5	5.9
GVM-3	N/A	4.8	8.0
GVM-5	N/A	8.0	8.0

(b) Scenario 2 (low-accuracy LEO)

	ECI	EqOE	J_2EqOE
EKF	8.6	86.7	> 100.8
UKF	11.1	92.7	> 100.8
GVM-3	N/A	92.7	> 100.8
GVM-5	N/A	> 100.8	> 100.8

(c) Scenario 3 (high-accuracy LEO)

	ECI	EqOE	J_2EqOE
EKF	2.6	> 30.0	> 30.0
UKF	3.0	> 30.0	> 30.0
GVM-3	N/A	> 30.0	> 30.0
GVM-5	N/A	> 30.0	> 30.0

(d) Scenario 4 (GEO)

	ECI	EqOE	J_2EqOE
EKF	0.6	4.6	> 14.0
UKF	0.6	4.6	> 14.0
GVM-3	N/A	4.6	> 14.0
GVM-5	N/A	8.6	> 14.0

(e) Scenario 5 (HEO)

Figure 1. Summary of uncertainty propagation results from Reference 9 for Scenarios 1–5. Listed in the tables are the number of orbital periods after which uncertainty realism breaks down (according to the Cramér-von Mises criterion with a confidence level of 99.9%) for a given combination of uncertainty propagation method and coordinate system used to represent the state PDF.

A. Simulation Setup

The test cases correspond to those presented in Reference 9, but we restrict our attention to uncertainty propagation via the prediction step of the unscented Kalman filter in which the propagated PDF is represented by a multi-variate Gaussian. We do not consider the prediction step of the extended Kalman filter (that was shown to be inferior to the UKF) nor that of the Gauss von Mises filter (that was shown to be superior to the UKF). Further, for Scenario 1 and Scenario 2 we shorten the timespan of propagation to 6 orbital periods, above which a single-component Gaussian mixture filter (i.e., a single UKF) in J_2EqOE would be insufficient. Full details of the procedure are described below.

1. Define an initial state and covariance at time t_0 by selecting one of the scenarios listed in Table 2. The test cases include objects in low Earth orbit (LEO), geostationary Earth orbit (GEO), and highly elliptical orbit (HEO).

2. Select an orbital element coordinate system in which to represent uncertainty, such as the traditional equinoctial orbital elements (EqOE), or the J_2 equinoctial orbital elements (J_2EqOE). If the state and covariance in Step 1 are not in this coordinate system, convert it to the targeted coordinate system using, for example, the unscented transform[c]. Here, we use J_2EqOE so that only a single Gaussian is needed at epoch and over the propagation times considered[d].

3. Select a particular (deterministic) dynamical model governing the perturbed two-body dynamics. The inclusion of at least J_2 dynamics is recommended.

4. Select propagation times $t_1, \ldots, t_M$ at which to perform the testing. The final time t_M should be

[c] Even for the low accuracy initial covariances in Table 3, this transformation does not result in loss of realism, as demonstrated in the results of Reference 9.

[d] Alternatively, one could use a Gaussian mixture in orbital elements during propagation and transform each component to a Gaussian mixture in Cartesian space. Without loss of generality, we consider the case in which a single Gaussian in J_2EqOE is sufficient. Methods for assessing the realism of a propagated Gaussian distribution are presented in References 9 and 10.

Table 2. Initial orbital states, with respect to (osculating) Keplerian orbital elements, used in the uncertainty propagation testing. The state covariances corresponding to the low, medium, and high accuracy cases are listed in Table 3. Depending on the scenario, the orbit and its uncertainty are propagated for 0.42, 7, or 30 days, beginning on 1 January 2008.

Scenario	Orbit Type	Orbit Accuracy	a (km)	e	i (°)	Ω (°)	ω (°)	M (°)	Timespan (days)
1	LEO	Low	7136.6	0.00949	72.9	116.0	57.7	105.5	0.42
2	LEO	Low	7136.6	0.0	0.0	0.0	0.0	0.0	0.42
3	LEO	High	7136.6	0.00949	72.9	116.0	57.7	105.5	7
4	GEO	Medium	42164.1	0.0	0.0	0.0	0.0	250.0	30
5	HEO	Medium	26628.1	0.742	63.4	120.0	0.0	144.0	7

Table 3. Parameters of the initial covariances used in the uncertainty propagation testing. The orbital state initial conditions are listed in Table 2. A covariance matrix $\mathbf{P}$ with respect to equinoctial orbital elements is constructed from a row in the table according to $\mathbf{P} = \mathbf{A}\mathbf{A}^T$, where $\mathbf{A} = \mathrm{diag}(\sigma_a, \sigma_h, \sigma_k, \sigma_p, \sigma_q, \sigma_\ell)$. Note that $1'' \doteq 4.848 \cdot 10^{-6}$ radians.

Orbit Accuracy	σ_a (m)	σ_h	σ_k	σ_p	σ_q	σ_ℓ
Low	20000	10^{-3}	10^{-3}	10^{-3}	10^{-3}	$36''$
Medium	2000	10^{-4}	10^{-4}	10^{-4}	10^{-4}	$28''$
High	50	10^{-5}	10^{-5}	10^{-5}	10^{-5}	$20''$

sufficiently large so as to necessitate the use of Gaussian mixtures. Note that sampling only at multiples of the orbital period is discouraged.

5. For $j = 1, \ldots, M$:

   (a) Propagate the PDF in Step 1 from time t_0 to t_j using the prediction step of the UKF in conjunction with the dynamical model specified in Step 3.

   (b) Sample random particle states, $\boldsymbol{y}^{(i)}(t_j)$, $i = 1, \ldots, k$, from the PDF obtained in Step 5(a),[e] and convert each point to Cartesian coordinates to obtain $\boldsymbol{x}^{(i)}(t_j)$, $i = 1, \ldots, k$.

   (c) Transform the propagated Gaussian in orbital elements from Step 5(a) to a Gaussian mixture p_x in Cartesian space using the approach outlined in Section II.

   (d) For $i = 1, \ldots, k$, evaluate the generalized uncertainty realism metric $\mathcal{U}_j^{(i)}$ defined in Section II, Subsection D:

$$\mathcal{U}_j^{(i)} = -2 \ln \left[\frac{p_x(\boldsymbol{x}^{(i)}(t_j); \boldsymbol{\Theta})}{p_x(\hat{\boldsymbol{x}}; \boldsymbol{\Theta})} \right],$$

   where $\boldsymbol{x}^{(i)}(t_j)$ is obtained from Step 5(b), and where $\hat{\boldsymbol{x}}$ is the mode of the Gaussian mixture p_x in Cartesian space obtained in Step 5(c).

   (e) Using the samples $\mathcal{U}_j^{(i)}$ computed in Step 5(d), compute the Cramér-von Mises (CVM) test statistic,

$$Q_k = \frac{1}{12k} + \sum_{i=1}^{k} \left[\frac{2i-1}{2k} - F(z_j^{(i)}) \right]^2, \tag{9}$$

   where $z_j^{(i)}$, $i = 1, \ldots, k$, are the observed samples $\mathcal{U}_j^{(i)}$ in increasing order, and where $F(z)$ is the cumulative distribution function (CDF) of the chi-squared distribution with six degrees of

[e] For the case of a multivariate Gaussian with mean $\boldsymbol{\mu}$ and covariance $\mathbf{P}$, a random draw $\boldsymbol{x}$ can be obtained as follows. Let $\boldsymbol{z}$ be a vector where each component is an independent random draw from the standardized Gaussian (i.e., the Gaussian with mean 0 and variance 1); this functionality is provided in most programming languages and scientific and statistical software. Then, the required $\boldsymbol{x}$ is the vector $\boldsymbol{\mu} + \mathbf{A}\boldsymbol{z}$, where $\mathbf{A}$ is the lower-triangular Cholesky factor[22] of the covariance $\mathbf{P}$ such that $\mathbf{P} = \mathbf{A}\mathbf{A}^T$.

freedom:

$$F(z) = \begin{cases} 1 - \frac{1}{8}\mathrm{e}^{-z/2}(z^2 + 4z + 8), & z > 0, \\ 0, & \text{otherwise.} \end{cases}$$

Further details and our reasons for recommending the CVM test statistic are provided in Reference 10. Table 4 provides one-sided confidence intervals for the Cramér-von Mises test statistic for common significance levels and sample sizes k.

(f) If the Cramér-von Mises test statistic (9) computed in Step 5(e) pierces a 99.9% confidence interval (or some other confidence interval), generate a higher-fidelity Gaussian mixture representation of the state PDF than what was previously computed in Step 5(c), re-compute the samples $\mathcal{U}_j^{(i)}$, and re-evaluate the Cramér-von Mises test statistic. Repeat until the test statistic falls within the confidence interval, and record the number of Gaussian mixture components necessary to achieve uncertainty realism. Note that "truth" is not needed in this approach.

The dynamical models used in this testing are comprised of the following forces. For the objects in LEO, a degree and order 32 Earth gravity model is used, together with lunar-solar perturbations. For the object in GEO, a degree and order 8 Earth gravity model is used, together with lunar-solar perturbations and a nominal solar radiation pressure ballistic coefficient (SRPBC) of 0.1 m^2/kg. For the object in HEO, a degree and order 32 Earth gravity model is used, together with lunar-solar perturbations and a nominal SRPBC of 0.1 m^2/kg. Note that one could include stochastic accelerations (i.e., process noise) in the simulations, but because the stochastic accelerations are much smaller in magnitude than the deterministic accelerations, we do not expect the results to differ substantially nor the overall conclusions to change.

Table 4. One-sided confidence intervals for the Cramér-von Mises test statistic (9) for common significance levels and sample sizes k. Reproduced from Reference 23.

	One-Sided Confidence Interval for the Cramér-von Mises test statistic			
k	90%	95%	99%	99.9%
10	[0.008333, 0.34510]	[0.008333, 0.45441]	[0.008333, 0.71531]	[0.008333, 1.07428]
20	[0.004167, 0.34617]	[0.004167, 0.45778]	[0.004167, 0.72895]	[0.004167, 1.11898]
50	[0.001667, 0.34682]	[0.001667, 0.45986]	[0.001667, 0.73728]	[0.001667, 1.14507]
200	[0.000417, 0.34715]	[0.000417, 0.46091]	[0.000417, 0.74149]	[0.000417, 1.15783]
1000	[0.000083, 0.34724]	[0.000083, 0.46119]	[0.000083, 0.74262]	[0.000083, 1.16120]
∞	[0, 0.34730]	[0, 0.46136]	[0, 0.74346]	[0, 1.16204]

B. Simulation Results

We now present some results in which uncertainty is propagated in orbital elements and transformed to Cartesian space without loss of realism by applying the testing and simulation framework delineated in Section III, Subsection A. In addition to the initial states and covariances defined in Tables 2 and 3 and the dynamical models described at the end of Section III, Subsection A, one thousand Monte-Carlo samples ($k = 1000$) were used in the testing in conjunction with the authors' variable-step Gauss-Legendre implicit Runge-Kutta-based orbital propagator[14,15,16] used to propagate the uncertainties in Step 5(a).

The uncertainty propagation/realism test results are presented in Figures 2–6. Each figure contains three curves. The colors denote the different coordinate systems used for representing uncertainty: **red** for Cartesian ECI coordinates[f], **green** for EqOE, and **blue** for J_2EqOE. A number of observations can be made.

1. In all test cases, uncertainty realism can be maintained if a sufficient number of (Gaussian) mixture components are used.

[f]Conceivably, the tests described in this section could be performed in other systems of Cartesian coordinates, such as the perifocal PQW coordinates or the RSW or NTW satellite coordinate systems.[24] However, because any two Cartesian frames are related by an affine transformation (i.e., a rotation and translation), the same results would be obtained if we used a different Cartesian coordinate system.

2. Initially, only a single Gaussian is needed to maintain uncertainty realism based on the CVM test with a 99.9% confidence level. As the propagation time increases, the use of Gaussian mixtures is eventually needed to maintain uncertainty realism (even when using J_2EqOE).

3. In all cases, only a single Gaussian is needed to maintain uncertainty realism when uncertainty is represented in J_2EqOE coordinates (up to the maximum propagation time considered). Conversely, hundreds of mixture components are needed when using Cartesian coordinates to represent uncertainty.

4. The number of mixture components needed when using EqOE is always greater than or equal the number needed when using J_2EqOE, and always less than or equal to the number needed when using Cartesian coordinates.

5. The number of mixture components needed to maintain uncertainty realism increases linearly with increasing propagation time with a slope and intercept that depends on the initial state, covariance, and coordinate system used to represent uncertainty (as well as the chosen dynamical model).

6. In Scenarios 1 and 2 (low-accuracy LEOs), uncertainty realism is maintained in Cartesian coordinates using a single component below 1/4 of an orbital period, after which approximately 100 additional components are needed every orbital period. When using EqOE coordinates, a single component can be safely used up to 1.5 to 2.0 orbital periods, after which approximately 12 additional components are needed every orbital period. A single component in J_2EqOE is sufficient up to 6 orbital periods in both cases.

7. In Scenarios 3 and 4 (high-accuracy LEO and GEO), a single Gaussian in EqOE or J_2EqOE is sufficient. Over 350 Gaussians are needed when using Cartesian coordinates if uncertainty realism is to be maintained for 7 days for the high-accuracy LEO scenario and 30 days for the GEO scenario.

8. In Scenario 5 (HEO), a substantial increase in the number of mixture components occurs when the object nears perigee. After seven days of propagation, 350 components are needed when using Cartesian coordinates, 100 components are needed when using EqOE, and 1 component is needed when using J_2EqOE to represent uncertainty.

9. Except for very-short propagation times, the transformation of uncertainty in orbital elements to Cartesian space necessitates the use of Gaussian mixtures. Otherwise loss of realism will occur, which can have an adverse effect on downstream SSA functions.

In summary, orbital-element-based coordinate systems are well-suited for nonlinear uncertainty propagation in the context of the perturbed two-body problem, and conversion to Cartesian space without loss of realism is not only possible but straightforward. From an efficiency standpoint, the use of orbital-element-based coordinate systems substantially reduces the computational cost of uncertainty propagation, even when the uncertainty needs to be transformed into Cartesian space. This is due to the fact that propagating N Gaussians through the nonlinear dynamics is approximately N times more expensive than propagating a single Gaussian, and that propagating a single Gaussian is much more expensive than refining a Gaussian into a Gaussian mixture.

IV. Conclusions

Given unlimited computational resources, one can maintain covariance (and uncertainty) realism in a space object's state indefinitely (e.g., by using a Gaussian mixture filter with an ever-increasing number of components). Given finite computation resources, our objective has been to maintain covariance (and uncertainty) realism for as long as possible given a Gaussian PDF at epoch. The ability to propagate uncertainty in orbital elements and transform the result to Cartesian space without loss of realism is key to achieving this goal because (i) orbital elements mitigate the departure from Gaussianity and thereby improve performance (e.g., necessitating fewer mixture components during propagation), and (ii) Cartesian representations of uncertainty are needed to meet the interface requirements of many existing space surveillance systems. In this paper, we demonstrated how a Gaussian (or Gaussian mixture) in orbital element space can be refined into a Gaussian mixture in Cartesian space. Statistically-based metrics were also presented to assess the realism of said transformation.

Simulation studies were performed to demonstrate the relative merits of different coordinate systems used for representing uncertainty, assuming a Gaussian distribution at epoch, and to demonstrate the transformation of uncertainty to Cartesian space without loss of realism. Particular attention was given to the number of mixture components needed to maintain uncertainty realism as a function of the initial state, covariance, and propagation time. For example, a typical low-accuracy low Earth orbit (with state uncertainty representative of an uncorrelated track) can be propagated realistically for 10 hours using a single Gaussian in J_2 equinoctial orbital elements and then (optionally) refined into a Gaussian mixture in Cartesian space at the final time. Alternatively, a 100-component Gaussian mixture in EqOE or a 600-component Gaussian mixture in Cartesian coordinates would be need to be propagated through the nonlinear dynamics to achieve uncertainty realism in the same situation. Because the computational cost of uncertainty propagation is much greater than that of refinement, in order to maintain covariance and uncertainty realism using Gaussian mixtures in Cartesian space would require roughly 600 times the computational resources, and using Gaussian mixtures in EqOE would require roughly 100 times the computational resources in this example[g].

Acknowledgments

The authors thank Alex Mont and Dan Lingenfelter for their assistance with the software implementation. This work was funded, in part, by a Phase II STTR from the Air Force Office of Scientific Research (FA9550-12-C-0034) and a grant from the Air Force Office of Scientific Research (FA9550-11-1-0248).

References

[1]Nielsen, P. D., Alfriend, K. T., Bloomfield, M. J., Emmert, J. T., Y. Guo, T. D. Maclay, J. G. M., Morris, R. F., Poore, A. B., Russell, R. P., Saari, D. G., Scheeres, D. J., Schonberg, W. P., and Sridharan, R., *Continuing Kepler's Quest: Assessing Air Force Space Command's Astrodynamics Standards*, National Academies Press, Washington, DC, 2012.

[2]Ristic, B., Arulampalam, S., and Gordon, N., *Beyond the Kalman Filter: Particle Filters for Tracking Applications*, Artech House, Boston, 2004.

[3]Ito, K. and Xiong, K., "Gaussian filters for nonlinear filtering problems," *IEEE Transactions on Automatic Control*, Vol. 45, No. 5, 2000, pp. 910–927.

[4]Terejanu, G., Singla, P., Singh, T., and Scott, P. D., "Uncertainty propagation for nonlinear dynamic systems using Gaussian mixture models," *Journal of Guidance, Control and Dynamics*, Vol. 31, No. 6, 2008, pp. 1623–1633.

[5]Horwood, J. T., Aragon, N. D., and Poore, A. B., "Gaussian sum filters for space surveillance: theory and simulations," *Journal of Guidance, Control, and Dynamics*, Vol. 34, No. 6, 2011, pp. 1839–1851.

[6]Horwood, J. T. and Poore, A. B., "Adaptive Gaussian sum filters for space surveillance," *IEEE Transactions on Automatic Control*, Vol. 56, No. 8, 2011, pp. 1777–1790.

[7]DeMars, K. J., Bishop, R. H., and Jah, M. K., "A splitting Gaussian mixture method for the propagation of uncertainty in orbital mechanics," *Proceedings of the 21st AAS/AIAA Space Flight Mechanics Meeting*, New Orleans, LA, February 2011, Paper AAS-11-201.

[8]DeMars, K. J., Jah, M. K., Cheng, Y., and Bishop, R. H., "Methods for splitting Gaussian distributions and applications within the AEGIS filter," *Proceedings of the 22nd AAS/AIAA Space Flight Mechanics Meeting*, Charleston, SC, February 2012, Paper AAS-12-261.

[9]Horwood, J. T., Aristoff, J. M., Singh, N., and Poore, A. B., "A comparative study of new non-linear uncertainty propagation methods for space surveillance," *SPIE Proceedings: Signal and Data Processing of Small Targets 2014*, edited by O. E. Drummond, Vol. 9092, 2014.

[10]Horwood, J. T., Aristoff, J. M., Singh, N., Poore, A. B., and Hejduk, M. D., "Beyond covariance realism: a new metric for uncertainty realism," *SPIE Proceedings: Signal and Data Processing of Small Targets 2014*, edited by O. E. Drummond, Vol. 9092, 2014.

[11]Aristoff, J. M., Horwood, J. T., and Poore, A. B., "Non-singular J2 equinoctial orbital elements for improved uncertainty propagation," In Preparation.

[12]Horwood, J. T. and Poore, A. B., "Orbital state uncertainty realism," *Proceedings of the Advanced Maui Optical and Space Surveillance Technologies Conference*, Wailea, HI, September 2012.

[13]Horwood, J. T. and Poore, A. B., "Gauss von Mises distribution for improved uncertainty quantification in space situational awareness," *SIAM Journal of Uncertainty Quantification*, 2014, (To Appear).

[14]Aristoff, J. M., Horwood, J. T., and Poore, A. B., "Orbit and uncertainty propagation: a comparison of Gauss-Legendre-, Dormand-Prince-, and Chebyshev-Picard-based approaches," *Celestial Mechanics and Dynamical Astronomy*, Vol. 118, 2014, pp. 13–28.

[g]The computational cost can be reduced by roughly a factor of two by using an adaptive Gaussian mixture filter, as evidenced by the linear growth in the number of mixture components as a function of propagation time in the test cases. However, this assumes that the (near)-optimal refinement direction and times at which to refine the PDF are known a-priori or can be estimated efficiently.

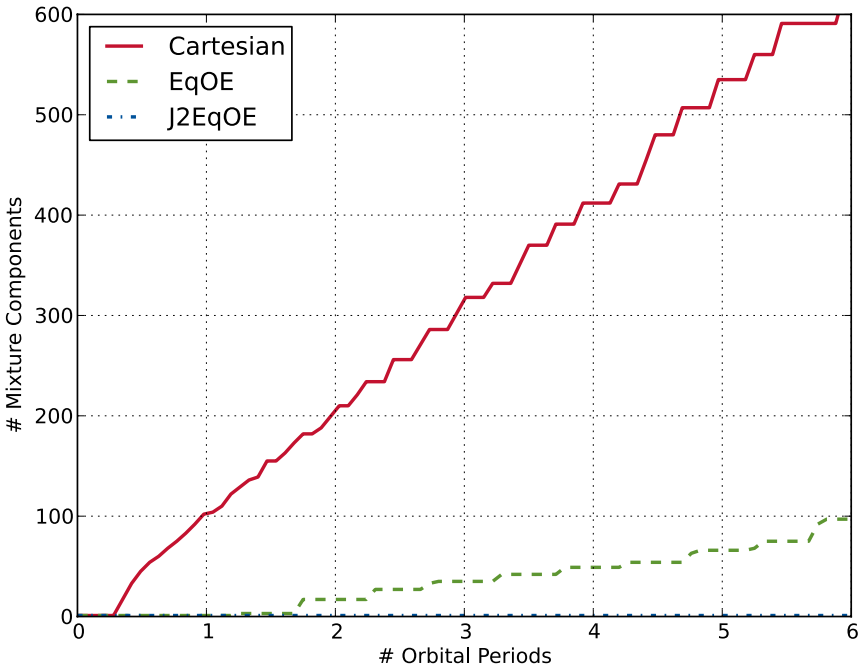

Figure 2. Number of Gaussian mixture components needed to achieve uncertainty realism in Scenario 1 (low-accuracy LEO) based on the CVM test with 99.9% confidence when the state uncertainty is represented in Cartesian (red) EqOE (green) and J_2EqOE (blue), and when the state PDF is propagated for 6 orbits.

[15]Aristoff, J. M., Horwood, J. T., Singh, N., and Poore, A. B., "Error estimation and control for efficient and reliable orbit (and uncertainty) propagation," *Proceedings of the 24th AAS/AIAA Space Flight Mechanics Meeting*, Santa Fe, NM, January 2014, Paper AIAA 2014-346.

[16]Aristoff, J. M., Horwood, J. T., and Poore, A. B., "Implicit Runge-Kutta-based methods for fast, precise, and scalable uncertainty propagation," 2014, (Under Review).

[17]Broucke, R. A. and Cefola, P. J., "On the equinoctial orbit elements," *Celestial Mechanics*, Vol. 5, 1972, pp. 303–310.

[18]Alspach, D. and Sorenson, H., "Nonlinear Bayesian estimation using Gaussian sum approximations," *IEEE Transactions on Automatic Control*, Vol. 17, No. 4, 1972, pp. 439–448.

[19]DeMars, K. J., *Nonlinear orbit uncertainty prediction and rectification for space situational awareness*, Ph.D. thesis, University of Texas at Austin, 2010.

[20]Julier, S. J., Uhlmann, J. K., and Durant-Whyte, H. F., "A new method for the nonlinear transformation of means and covariances in filters and estimators," *IEEE Transactions on Automatic Control*, Vol. 55, 2000, pp. 477–482.

[21]Mahalanobis, P. C., "On the generalised distance in statistics," *Proceedings of the National Institute of Sciences of India*, Vol. 2, No. 1, 1936, pp. 49–55.

[22]Golub, G. and Van Loan, C., *Matrix Computations*, John Hopkins University Press, Baltimore, MD, 1996.

[23]Csörgö, S. and Faraway, J. J., "The exact and asymptotic distributions of the Cramér-von Mises statistics," *Journal of the Royal Statistical Society Series B*, Vol. 58, No. 1, 1996, pp. 221–234.

[24]Vallado, D. A., *Fundamentals of Astrodynamics and Applications*, Springer, New York, 2007.

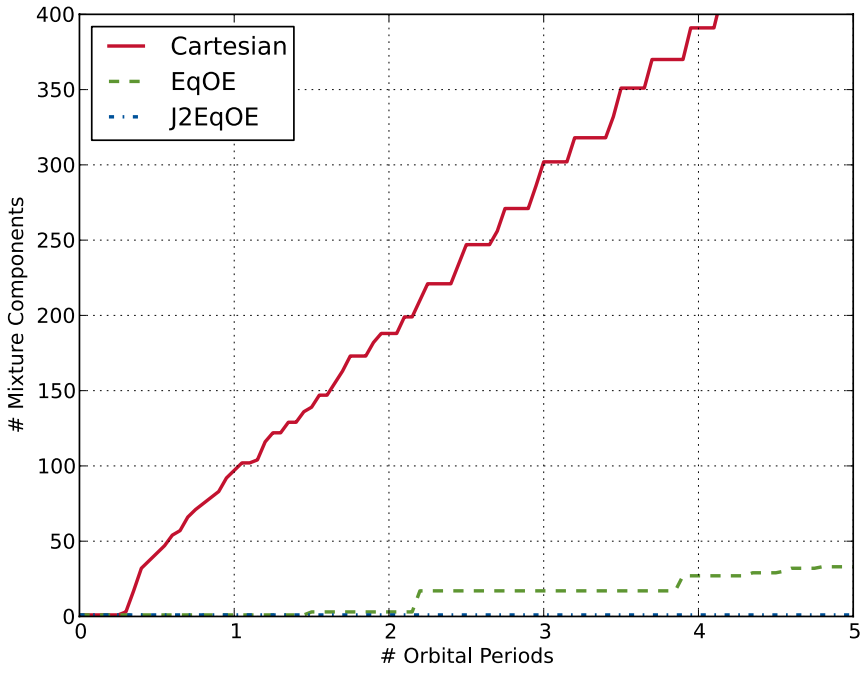

Figure 3. Number of Gaussian mixture components needed to achieve uncertainty realism in Scenario 2 (low-accuracy LEO) based on the CVM test with 99.9% confidence when the state uncertainty is represented in Cartesian (red) EqOE (green) and J_2EqOE (blue), and when the state PDF is propagated for 5 orbits.

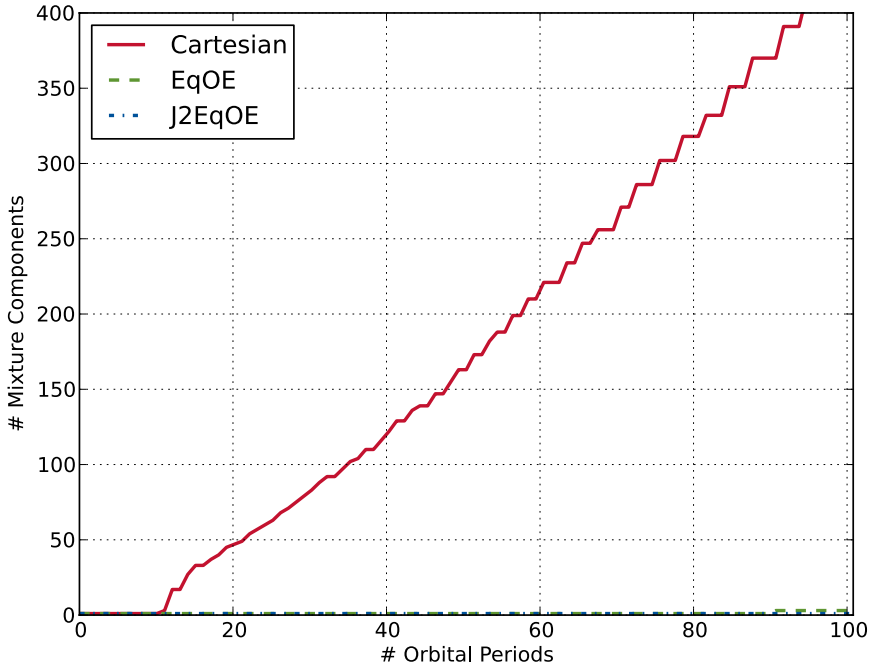

Figure 4. Number of Gaussian mixture components needed to achieve uncertainty realism in Scenario 3 (high-accuracy LEO) based on the CVM test with 99.9% confidence when the state uncertainty is represented in Cartesian (red) EqOE (green) and J_2EqOE (blue), and when the state PDF is propagated for 7 days.

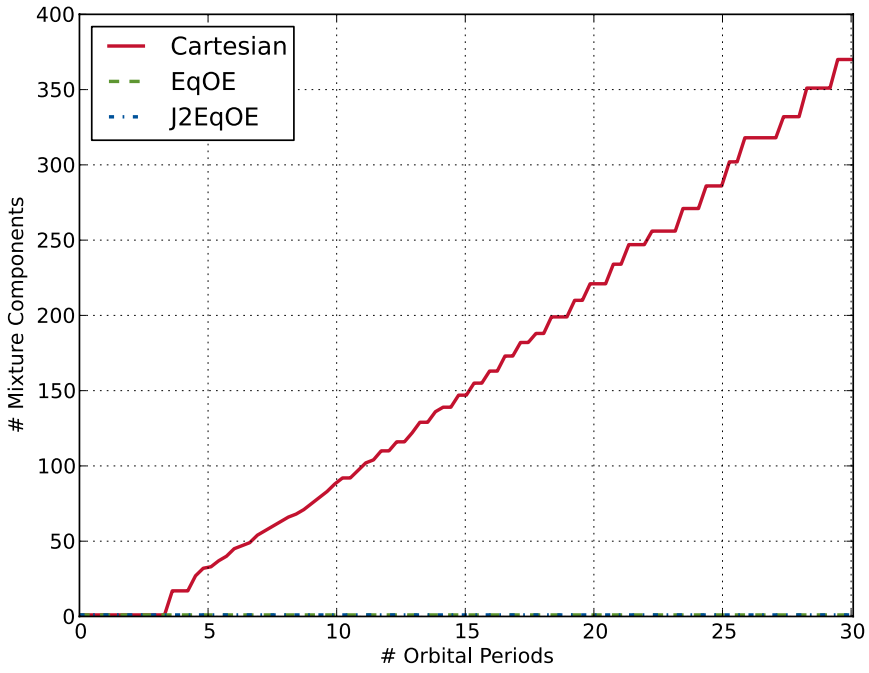

Figure 5. Number of Gaussian mixture components needed to achieve uncertainty realism in Scenario 4 (GEO) based on the CVM test with 99.9% confidence when the state uncertainty is represented in Cartesian (red) EqOE (green) and J_2EqOE (blue), and when the state PDF is propagated for 30 days.

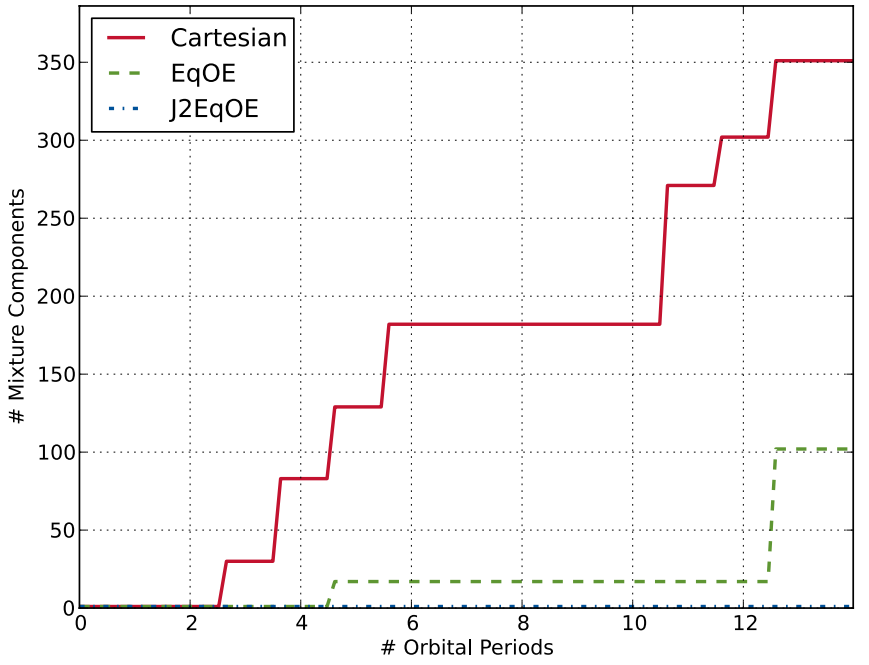

Figure 6. Number of Gaussian mixture components needed to achieve uncertainty realism in Scenario 5 (HEO) based on the CVM test with 99.9% confidence when the state uncertainty is represented in Cartesian (red) EqOE (green) and J_2EqOE (blue), and when the state PDF is propagated for 7 days.